



# Halotherapy relieves chronic obstructive pulmonary disease by alleviating NLRP3 inflammasome-mediated pyroptosis

Chenyan Zhang<sup>1#</sup>, Weijie Zhu<sup>1#</sup>, Qinghai Meng<sup>1</sup>, Naqi Lian<sup>1</sup>, Jingzhen Wu<sup>1</sup>, Bowen Liu<sup>1</sup>, Hao Wang<sup>1</sup>, Xinyu Wang<sup>2</sup>, Shujun Gu<sup>2</sup>, Jingli Wen<sup>2</sup>, Xiaoling Shen<sup>3</sup>, Yu Li<sup>1</sup>, Xu Qi<sup>2,4</sup>

<sup>1</sup>School of Medicine & Holistic Integrative Medicine, Nanjing University of Chinese Medicine, Nanjing, China; <sup>2</sup>Department of Respiratory Medicine, The First Affiliated Hospital of Nanjing Medical University, Nanjing, China; <sup>3</sup>Nanjing Kuancheng Technology Co., Ltd., Nanjing, China; <sup>4</sup>The Affiliated Jiangsu Shengze Hospital of Nanjing Medical University, Suzhou, China

*Contributions:* (I) Conception and design: All authors; (II) Administrative support: Y Li, X Qi; (III) Provision of study materials or patients: Y Li, X Qi; (IV) Collection and assembly of data: C Zhang, W Zhu; (V) Data analysis and interpretation: C Zhang, W Zhu; (VI) Manuscript writing: All authors; (VII) Final approval of manuscript: All authors.

<sup>#</sup>These authors contributed equally to this work.

*Correspondence to:* Yu Li. School of Medicine & Holistic Integrative Medicine, Nanjing University of Chinese Medicine, Nanjing 210023, China. Email: liyu@njucm.edu.cn; Xu Qi. Department of Respiratory Medicine, The First Affiliated Hospital of Nanjing Medical University, Nanjing 210029, China; The Affiliated Jiangsu Shengze Hospital of Nanjing Medical University, Suzhou 210046, China. Email: qixuly@163.com.

**Background:** Airway remodeling and inflammation are considered the main characteristics of chronic obstructive pulmonary disease (COPD). Cigarette smoke promotes the occurrence of inflammation, oxidative stress, and pyroptosis. Halotherapy has been shown to dilute secretions in the airways and promote drainage, but the mechanism remains unclear. In this study, we evaluated the anti-inflammatory and antioxidant effects of halotherapy in COPD rats and investigated the underlying mechanism.

**Methods:** A COPD rat model was constructed by cigarette smoke and lipopolysaccharide tracheal instillation. A total of 120 male Sprague-Dawley (SD) rats were randomly divided into control, model, halotherapy, terbutaline, halotherapy + terbutaline, and Ac-YVAD-CMK (Caspase-1 inhibitor) groups. After modeling and treatment, the pulmonary function of the rats was measured. Pathological changes in the lungs were measured by hematoxylin-eosin (H&E) staining. Serum interleukin-1 $\beta$  (IL-1 $\beta$ ), tumor necrosis factor- $\alpha$  (TNF- $\alpha$ ), interleukin-4 (IL-4), and nitric oxide (NO) levels were determined using enzyme-linked immunosorbent assay (ELISA) kits. Malondialdehyde (MDA) levels and superoxide dismutase (SOD) activity in the lungs were determined by biochemical tests. The levels of cluster of differentiation 4 (CD4<sup>+</sup>) and CD8<sup>+</sup> T cells in the blood were determined by flow cytometry. The expression levels of Toll-like receptor 4 (TLR4), nuclear factor kappa B (NF- $\kappa$ B), gasdermin-D (GSDMD), nucleotide-binding oligomerization domain-like receptor protein 3 (NLRP3), apoptosis-associated speck-like protein containing a C-terminal caspase recruitment domain (ASC), Caspase-1, and IL-1 $\beta$  in lung tissues were detected by immunohistochemistry, Western blotting, or quantitative polymerase chain reaction (qPCR).

**Results:** Halotherapy recovered the clinical symptoms of COPD rats, and reduced lung inflammatory cell infiltration and air wall attenuation. It also relieved oxidative stress in the lung tissue of COPD rats, reduced CD4<sup>+</sup> and CD8<sup>+</sup> T cell accumulation in lung tissue, and decreased inflammatory factor production in the serum of COPD rats. Furthermore, it inhibited the TLR4/NF- $\kappa$ B/GSDMD and NLRP3/ASC/Caspase-1 signaling pathways. Ac-YVAD-CMK could not completely inhibit the therapeutic effect of halotherapy on COPD rats.

**Conclusions:** Halotherapy improves lung function by inhibiting the NLRP3/ASC/Caspase-1 signaling pathway to reduce inflammation and pyroptosis in COPD rats, and may be a new option for the prevention and treatment of COPD.

**Keywords:** Chronic obstructive pulmonary disease (COPD); halotherapy; pyroptosis; inflammation; oxidative stress

Submitted Oct 18, 2022. Accepted for publication Nov 29, 2022.

doi: 10.21037/atm-22-5632

View this article at: <https://dx.doi.org/10.21037/atm-22-5632>

## Introduction

Chronic obstructive pulmonary disease (COPD) is one of the most common preventable lung diseases and is characterized by persistent incompletely reversible airflow limitation. It is often associated with respiratory exposure to toxic particles and harmful gases causing chronic inflammatory responses (1) and affects more than 250 million people worldwide (2). Among the pathogenic mechanisms of COPD, chronic airway inflammation and oxidative stress play important roles. Such stimuli are divided into two types: endogenous oxidants are mainly derived from inflammatory cells (1), while exogenous oxidants are primarily derived from cigarette smoke and air pollution. Cigarette smoking (3) is considered a high-risk factor for COPD because of its damage caused by oxygen free radicals (4).

With an increasing smoking population, the prevalence and mortality of COPD are increasing every year, and it is expected that more than 4.5 million people will die from COPD annually by 2030 (5). These results in an important public health problem that severely affect the health and socioeconomic promotion of patients (6). The current clinical guidelines for the diagnosis and treatment of COPD (revised in 2021) regard pulmonary function testing as the golden standard for the diagnosis of COPD (7). At present, the overall goals of clinical treatment include symptomatic control, alleviating the condition, reducing exacerbations, and improving quality of life. Clinical mainstream use

of glucocorticoid,  $\beta_2$  agonist, and other adjuvant drugs, mostly by the use of combined drug delivery. However, the reversibility of airway obstruction caused by inflammation in COPD is low, and current drug treatments are not effective in delaying disease progression (8,9). Therefore, there is an urgent need to identify or develop novel treatment modalities with good efficacy and few toxic side effects for the prevention and treatment of COPD in terms of protecting lung function.

Clearing airway secretions is one of the important contents in the treatment of COPD. The biggest advantage of halotherapy is that it can remove the secretions in the deep airway and minimize the discomfort of patients. It works by physical means and avoids the side effects brought about by the drugs. This makes it easier for patients to accept. The effect of halotherapy in treating COPD has been proved in clinical practice, but there are few explanations about how it works in existing research. In the 2016 clinical trial, 73 patients with mild and moderate COPD were included and divided into the control group and the experimental group. According to the comprehensive evaluation of clinical manifestations and respiratory function laboratory data, the overall effective rate of mild to moderate patients is 95% and 80% (10). A recent review described how halotherapy improves patients' respiratory function and quality of life (11). However, it is not explicit how halotherapy works at the molecular level.

Pyroptosis is an enigmatic area in programmed cell death waiting to be explored. Its relationship with the disease is urgent to be known. The nucleotide-binding oligomerization domain-like receptor protein 3 (NLRP3)/apoptosis-associated speck-like protein containing a C-terminal caspase recruitment domain (ASC)/Caspase-1 pathway plays an important role in cigarette smoke-induced pyroptosis in bronchial epithelial cells (12). We therefore innovatively combined the two to make the hypothesis, whether halotherapy could reduce inflammation, immune and oxidative stress in COPD by acting on the NLRP3/ASC/Caspase-1 inflammatory pathway. Herein, we referred to previous studies to establish a COPD rat model (13-15), aiming to evaluate the effects of halotherapy on COPD rats. It is speculated that the down-regulation of NLRP3 inflammasome expression is an important

### Highlight box

#### Key findings

- Halotherapy improves lung function by inhibiting the NLRP3/ASC/Caspase-1 signaling pathway to reduce inflammation and pyroptosis in COPD rats.

#### What is known and what is new?

- Airway remodeling and inflammation are considered the main characteristics of COPD.
- Halotherapy can relieve COPD, but the mechanism remains unclear.

#### What is the implication, and what should change now?

- Halotherapy may be a new option for COPD.

regulatory mechanism of halotherapy. We present the following article in accordance with the ARRIVE reporting checklist (available at <https://atm.amegroups.com/article/view/10.21037/atm-22-5632/rc>).

## Methods

### *Experimental animals*

This study was conducted in accordance with internationally accepted animal welfare guidelines and passed the ethics review of Nanjing University of Chinese Medicine (No. 202007A015). A total of 120 male Sprague-Dawley (SD) rats (270±20 g, 8 weeks old) were purchased from Hangzhou Medical College [License No. SCXK(zhe)2019-0002; Zhejiang, China]. All rats were housed in a temperature-controlled animal facility with a 12-h light/dark cycle, with water and rodent chow provided *ad libitum*.

### *Modeling and treatment*

A protocol was prepared before the study without registration. COPD model establishment was based on the previous literature. The rats were randomly divided into a control group, model group, terbutaline group, halotherapy group, halotherapy + terbutaline group, and Ac-YVAD-CMK (Caspase-1 inhibitor) + halotherapy group, with 20 rats in each group. To avoid the influence of respiratory products on the experiment, the rats were housed separately in multiple cages. Except for the control group, all rats were injected with lipopolysaccharide (LPS) (Sigma, USA) 0.2 mL (1 mg/mL) via the trachea on the 1<sup>st</sup> and 14<sup>th</sup> days. The rats were then placed into a glass fumigating box on the 2<sup>nd</sup>–30<sup>th</sup> day (except for the 14<sup>th</sup> day) to smoke cigarettes [Hongmei cigarettes, Hongta Tobacco (Group) LLC, China; twice daily, 60 minutes to smoke 6 cigarettes each time]. We chose 84 mm flue-cured cigarettes; the amount of nicotine was 0.8 mg, the amount of tar was 10 mg, and the amount of carbon monoxide was 12 mg.

The Caspase-1 inhibitor, Ac-YVAD-CMK (ChemeGen Biotech Co., Ltd., China), was administered by intraperitoneal injection twice daily (dose: 0.3 mg/100 g rat body weight), and the drugs were configured using a 0.9% sodium chloride solution. Upon completion of the treatment, the rats were anesthetized with 2% sodium pentobarbital solution (2 mL/kg) and sacrificed by carotid artery exsanguination, and their plasma, serum, and lung tissue samples were collected. To guarantee the practice of

blinding, different personnel were assigned to perform the experiments and data analysis.

### *Lung function detection*

Ventilatory parameters were recorded continuously for 20 min (IOX2, EMKA Technologies, Paris). The awake rats were placed in a full-body volume tracking box, adapted to the environment for 10 min, and the situation was recorded for 10 min to measure the tidal volume (TV), expiratory volume (EV), relaxation time (RT), end-expiratory pause (EEP), pause-enhanced bronchial constriction (Penh), peak expiratory flow (PEF), peak inspiratory flow (PIF), minute ventilation volume (MV), expiratory flow rate at 50% TV (EF50), frequency of breathing (f), etc.

### *Morphological and histopathological assessment of lung tissue*

The left lung tissue of rats was immersed in 4% paraformaldehyde solution and embedded into wax blocks after routine dehydration, transparency, and wax immersion. The tissues were sliced into 5 µm sections after baking and soaked in xylene to remove the paraffin-embedded tissue. Hematoxylin-eosin (H&E) staining was then performed. Next, observation was performed at 400×, and photos were taken with an optical microscope (Nikon, Japan). The pathological changes in rat lung tissue were analyzed.

### *Immunohistochemical analysis*

After rehydration, rat lung tissue sections were immersed in a 3% hydrogen peroxide solution to inactivate the endogenous peroxidase. Next, the rat lung tissue sections were rinsed three times using phosphate buffered saline (PBS) buffer and were then placed in a preheated citrate buffer above 95 °C for 20 min of incubation, after which they were left at room temperature for 20 min for antigen retrieval. Tissue sections were first permeabilized using 0.2% Triton X-100 for 20 min at room temperature and then blocked for 30 min at room temperature using a 5% bovine serum albumin (BSA) solution overlaid in a moisturizing box for immunohistochemical staining. The rat lung tissues were covered by diluting antibodies according to the antibody instructions and rinsed three times using PBS buffer overnight at 4 °C.

Horseradish peroxidase (HRP)-modified secondary antibodies were diluted according to the antibody

instructions and overlaid onto the rat lung tissue for 2 h. The sections were washed three times using PBS buffer, washed three times with 3,3'-diaminobenzidine (DAB) chromogen working solution, and covered with rat lung tissue for color development. The color development was terminated using PBS rinsing of the specimen when the extent was sufficient. We then counterstained the nuclei with hematoxylin, and after differentiation with an ethanolic hydrochloride solution, tap water was blunted. Subsequently, the ethanol solution with an increasing concentration gradient was quickly dehydrated and soaked in xylene for 5 min. A neutral resin-blocking solution was used to cover the tissue, which was then covered with a coverslip. The sections were observed and photographed using a light microscope (Nikon, Japan). The expression changes of the target antibody in the rat lung tissues were analyzed.

#### *Superoxide dismutase (SOD) activity measurement*

Frozen lung tissue and normal saline were ground into 10% tissue homogenate on ice at a ratio of 1:9. A SOD Detection Kit (A001-3-2; Nanjing Jiancheng Bioengineering Institute, Nanjing, China) was selected for SOD measurement. The assay was conducted according to the manufacturer's instructions.

#### *Lipid peroxidation determination*

A malondialdehyde (MDA) Detection Kit (A003-1-2; Nanjing Jiancheng Bioengineering Institute, Nanjing, China) was selected to determine the MDA level as a marker of lipid peroxidation. The assay was conducted according to the manufacturer's instructions. The level of MDA was expressed as nanomoles per milligram protein.

#### *Nitric oxide (NO) concentration detection*

NO (vascular endothelial relaxation factor) generates nitrate and nitrite, and after generating light red azo compounds, the NO concentration can be indirectly measured by colorimetry. The assay was performed using a kit (A013-2-1; Nanjing Jiancheng Bioengineering Institute, Nanjing, China) according to the manufacturer's instructions.

#### *Enzyme-linked immunosorbent assay (ELISA)*

To evaluate the inflammatory response and therapeutic

effects in the rat COPD model, blood was collected from the carotid artery after the rats were anesthetized. The blood was collected in a centrifuge tube, placed at room temperature for 20 min, and then centrifuged at 3,000 r/min for 20 min to separate the serum. The levels of interleukin-1 $\beta$  (IL-1 $\beta$ ), interleukin-4 (IL-4), tumor necrosis factor- $\alpha$  (TNF- $\alpha$ ) were detected according to the protocol of the ELISA kit manufacturer (Mlbio, Shanghai, China).

#### *Lymphocytes detection by flow cytometry*

Rat plasma (6 mL) was collected using an ethylene diamine tetraacetic acid (EDTA) anticoagulant tube (BD Vacutainer, USA). The fluorescent antibody cluster of differentiation 4-fluorescein isothiocyanate isomer (CD4-FITC)/cluster of differentiation 8-phycoerythrin (CD8-PE) was added to the test tube, mixed well, incubated, hemolyzed, and washed before putting on the machine. The instructions of the instrument and reagents were followed strictly to determine the percentage of CD4<sup>+</sup> and CD8<sup>+</sup> T cells.

#### *Western blot*

Protein expression in the lung tissues was evaluated by Western blotting. Briefly, total protein extracts from the lung tissues were separated by polyacrylamide gradient gels (10%) and transferred to polyvinylidene fluoride membranes. The membranes were incubated overnight at 4 °C with primary antibodies, including Toll-like receptor 4 (TLR4), nuclear factor kappaB (NF- $\kappa$ B), gasdermin-D (GSDMD), NLRP3/ASC, Caspase-1 and  $\beta$ -actin antibodies. Next, the respective HRP-conjugated secondary antibodies were incubated for 2 hours, followed by three washes. The membranes were then incubated with electrochemiluminescence (ECL) (Biosharp, China) for luminescence generation. The image and gray level were analyzed with ImageLab and ImageJ software. The protein expression level was evaluated using the  $\beta$ -actin ratio.

#### *Quantitative polymerase chain reaction (qPCR)*

For total ribonucleic acid (RNA) extraction, the upper lobes of the right lung tissues (50 mg) were dissolved in TRIzol (1 mL) (Ambion, USA). RNA was reverse transcribed using TORO Blue<sup>®</sup> qRT Premix with gDNA Eraser kit (Toroivd, Shanghai, China). Agilent Technologies Stratagene Mx3000P (Agilent, USA) was

used to monitor the amplification reactions in real-time. The initial activation was at 95 °C for 15 s, 60 °C for 15 s, 72 °C for 45 s, and 40 cycles. The rat *caspase-1*, *gsdmd*, *nlrp3*, and *il-1 $\beta$*  primers used for PCR were as follows: 5'-AAACACCCACTCGTACACGTCTTG-3' (forward) and 5'-AGGTCAACATCAGCTCCGACTCTC-3' (reverse) for *caspase-1*; 5'-CAGCAGGCAGCATCCTTGAGTG-3' (forward) and 5'-CCTCCAGAGCCTTAGTAGCCAGTAG-3' (reverse) for *gsdmd*; 5'-CGTCTAGGTGAGAGCGTGGA-3' (forward) and 5'-ATGCTCCCTTTCCTGCTTGC-3' (reverse) for *nlrp3*; 5'-AATCTCACAGCAGCATCTCGACAAG-3' (forward) and 5'-TCCACGGGCAAGACATAGGTAGC-3' (reverse) for *il-1 $\beta$* ; 5'-TGTGGTGGAGGACTTGCTGAGG-3' (forward) and 5'-AGTGCTGCCTTGCTGTTCTTGAG-3' (reverse) for *nf- $\kappa$ b*; and 5'-GACATGCCGCCTGGAGAAAC-3' (forward) and 5'-AGCCCAGGATGCCCTTTAGT-3' (reverse) for *gapdh*. The values of the target genes were normalized using the value of the *gapdh* housekeeping gene. All samples were run in triplicate, and the average values were calculated.

### Statistical analyses

All experiments were performed in triplicate, and all measurements are presented as the mean  $\pm$  standard error of the mean (SEM). Differences between multiple groups were analyzed by one-way analysis of variance (ANOVA), and multiple comparisons between groups were assessed with *post-hoc* tests using a *t*-test. Differences were considered significant when  $P < 0.05$ . All of the above mapping statistics and analyses were performed using GraphPad Prism 8.0 (GraphPad, USA).

## Results

### Halotherapy improves the pulmonary pathology of COPD rats

Figure 1A displays the flow chart of modeling and drug administration of COPD rats. Two weeks after modeling, the rats developed cough symptoms. After 3 weeks, the rats developed rapid wheezing, hunchback, and even hair loss. In addition, rats in the control group had no cough symptoms, and their hair was relatively shiny. After 1 week of administration, the cough symptoms of rats in the terbutaline group were gradually relieved, and the coat color gradually returned to normal after 1 month of halotherapy. Weight gain could partly reflect the health of rats. Based on our monthly weight data collection, halotherapy was found

to ameliorate the slow weight gain caused by smoking cigarettes (Figure 1B).

The H&E staining results showed that the alveolar structure and tracheal morphology of rats in the control group were intact. Pseudostratified ciliated columnar epithelial cells were neatly arranged, and the goblet cells were uniform in size. After exposure to cigarettes, the alveoli of the model group rats collapsed and fused. This is accompanied by the characteristic changes of emphysema, including thickening of the bronchiolar and pulmonary vessel walls and bronchial lumen stenosis. At the same time, the surrounding glands were enlarged, and there was inflammatory cell accumulation around the bronchioles in rats with cigarette smoke. The above-mentioned pathological changes in the trachea and lung tissue were consistent with those observed in clinical COPD patients, providing strong evidence for evaluating whether the animal model met the conditions of COPD (15). In the terbutaline group, the tracheal lumen recovered well but the bullae did not improve. In the halotherapy group, the degree of glandular hypertrophy was reduced, lumen stenosis was improved, and the infiltration of surrounding inflammatory cells was reduced (Figure 1C).

### Halotherapy improves respiratory function in COPD rats

Pulmonary function tests and pathological examinations are two key methods of evaluating the modeling of COPD animals (16). Pulmonary function examination is the main objective indicator of airflow limitation. In the study, the pulmonary function test indexes showed that TV, EV, EEP, and Penh were increased, while MV, PIF, EF50, and f were decreased in rats with cigarette smoke, as compared to the control group (Figure 2). These results indicated that expiratory resistance increased, the residual volume of the lungs increased, lung capacity decreased, and lung compliance decreased in rats with cigarette smoke, indicating the existence of obstructive ventilation disorders. The TV, EV, EEP, and Penh pulmonary function indexes of the rats were improved after halotherapy treatment, demonstrating that halotherapy improves lung damage in COPD rats (Figure 2).

### Halotherapy suppresses oxidative stress in COPD rats

When COPD occurs, the ability of SOD to scavenge oxygen free radicals is reduced, resulting in the

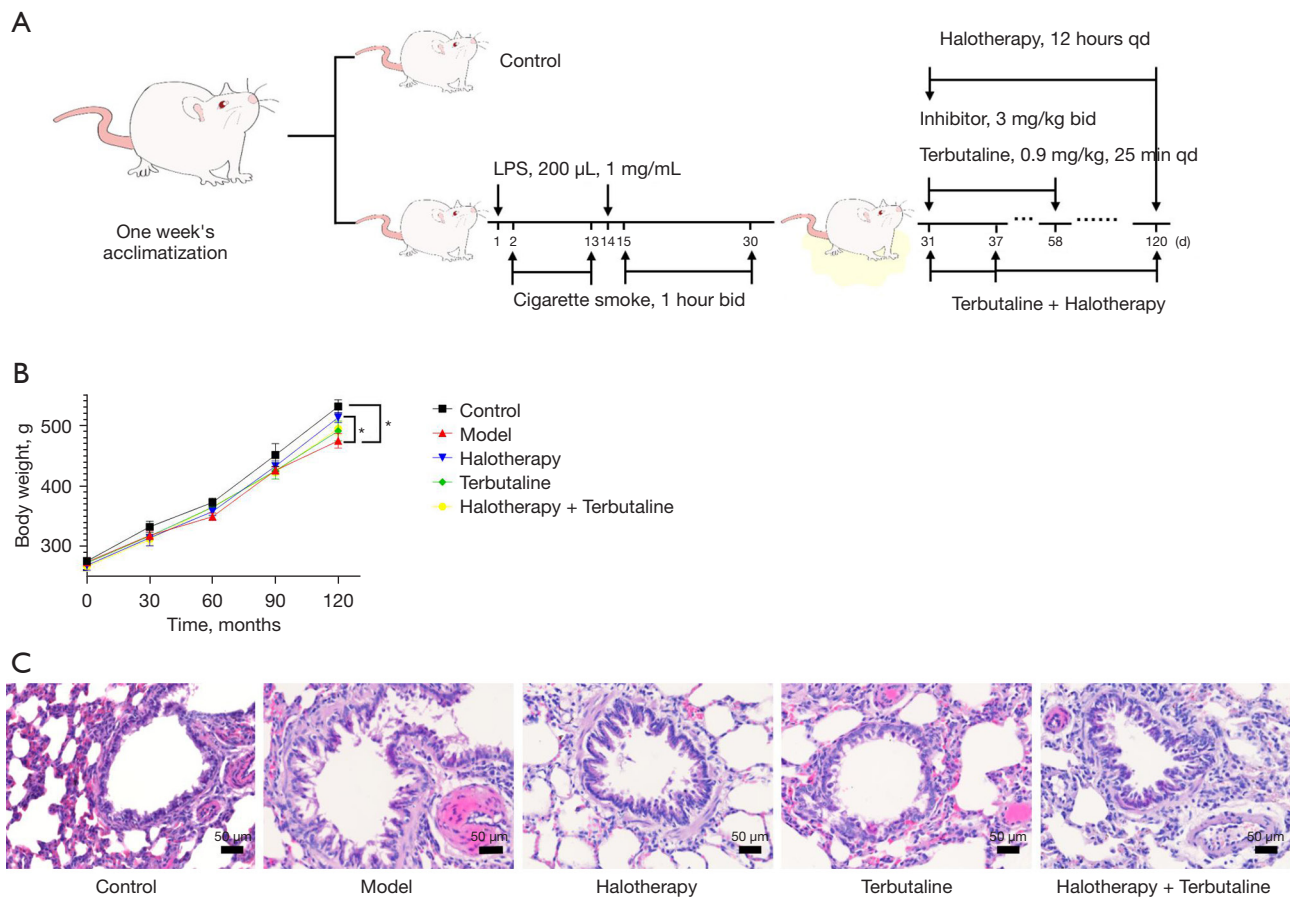


**Figure 1** Halotherapy improves the pulmonary pathology in COPD rats. (A) Flow chart showing the experimental design. (B) The changes in body weight of each group were reported every month. (C) Pulmonary histology was detected by H&E staining (scale bar, 50  $\mu$ m). Data are expressed as the mean  $\pm$  SEM. One-way ANOVA was adopted for statistical analysis. \*,  $P < 0.05$  compared with the model group ( $n = 8$ ). LPS, lipopolysaccharide; qd, once per day; bid, twice per day; COPD, chronic obstructive pulmonary disease; H&E, hematoxylin and eosin; SEM, standard error of the mean; ANOVA, analysis of variance.

accumulation of oxygen free radicals, damage to the biological function of alveolar cell membranes, cell damage and aging, enhanced oxidative stress, as well as increased production of MDA and other toxic substances. Compared with the control group, the COPD rats showed decreased SOD activity and increased MDA levels in the lungs. After halotherapy treatment, SOD activity was remarkably increased, while the MDA level was significantly decreased in the lungs of COPD rats (Figure 3A,3B), which indicated that oxidative stress in the development of COPD could be improved by halotherapy. Inducible nitric oxide synthase (iNOS) produces NO, which is associated with blood pressure regulation, inflammation, and infection (17). NO is involved in the regulation of various signaling pathways

related to transcription factor activation and gene expression as well as in the post-translational regulation of the activity of various inflammatory mediators. The effects of its activation and reflection are complex (18). Compared with the control group, the COPD rats showed decreased NO levels in the lungs, which could be reduced by halotherapy treatment. Also, iNOS protein expression in lung tissues showed consistent changes to NO levels in the COPD rats (Figure 3C,3D).

#### *Halotherapy alleviates inflammation and the immune response in COPD rats*

Inflammation is the central mechanism of COPD

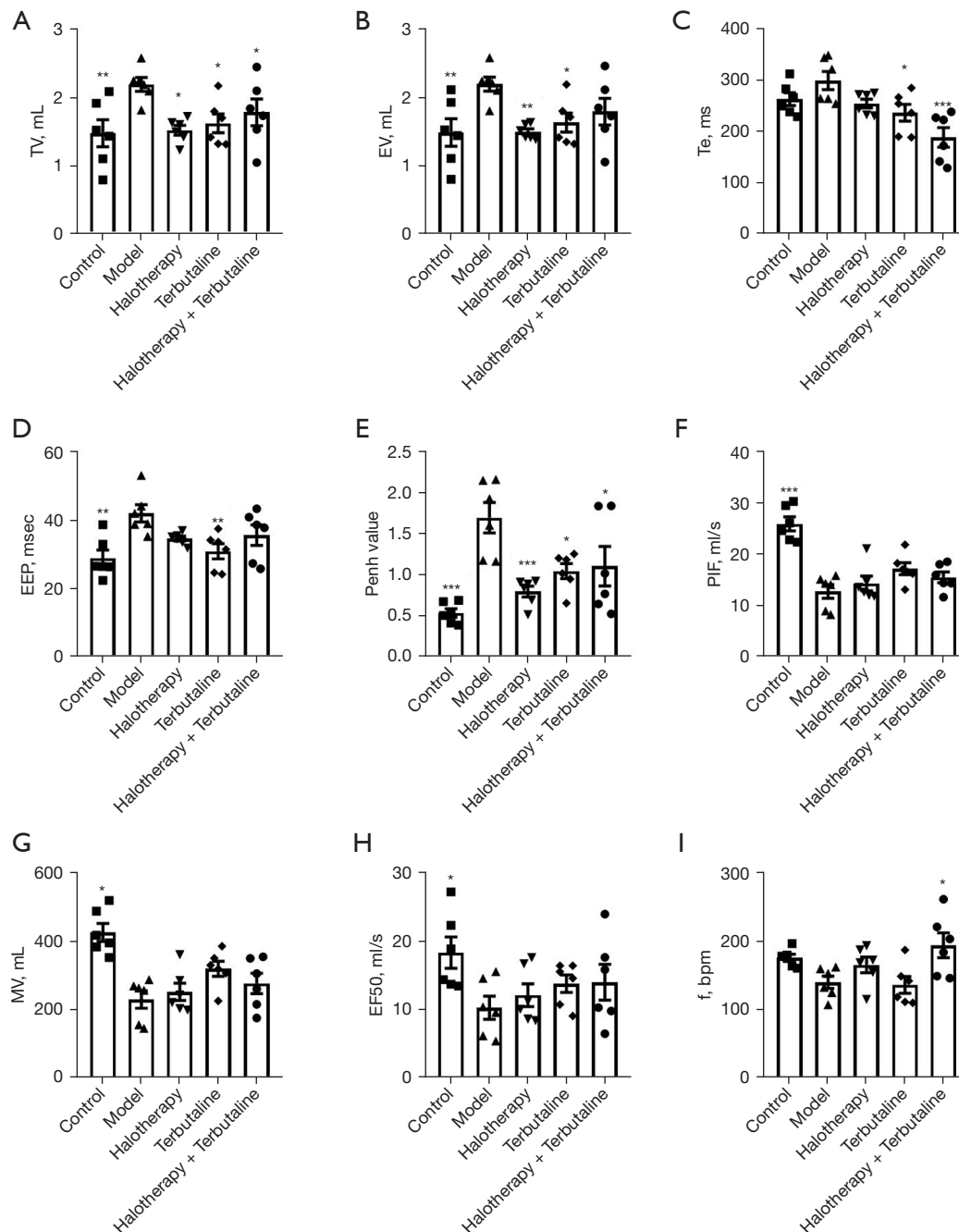


**Figure 2** Halotherapy improves respiratory function in COPD rats. The following indexes were recorded by pulmonary function test in rats: TV (A), EV (B), Te (C), EEP (D), Penh (E), PIF (F), MV (G), EF50 (H), and f (I). Data are expressed as the mean  $\pm$  SEM. One-way ANOVA was adopted for statistical analysis. \*,  $P < 0.05$ ; \*\*,  $P < 0.01$ ; \*\*\*,  $P < 0.001$  compared with the model group (n=6). TV, tidal volume; EV, expiratory volume; Te, expiration duration; EEP, end-expiratory pause; Penh, enhanced pause; PIF, maximum inspiratory flow; MV, inspiratory capacity per minute; EF50, 50% exhaled volume flow rate; f, breath rate; COPD, chronic obstructive pulmonary disease; SEM, standard error of the mean; ANOVA, analysis of variance.

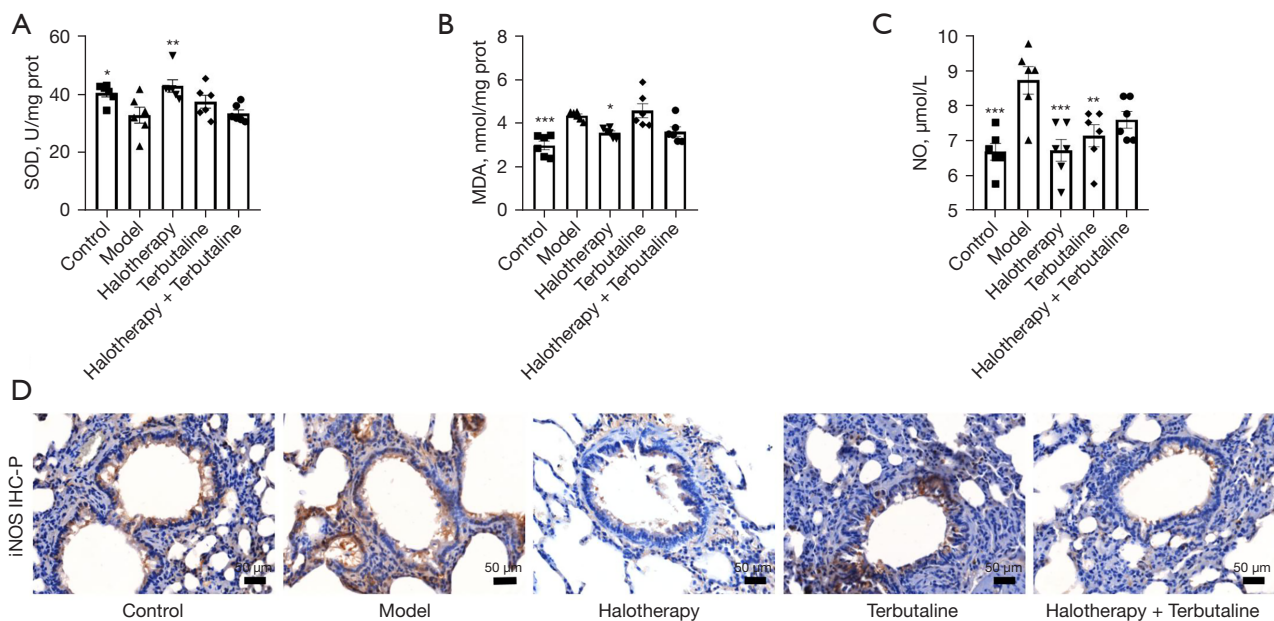


**Figure 3** Halotherapy suppresses oxidative stress in COPD rats. (A,B) SOD activity (A) and MDA concentration (B) in the lung tissue homogenates. (C) NO levels in the serum were detected using biochemical kits. (D) The protein expression of iNOS was detected by immunohistochemistry (scale bar, 50 µm). Data are expressed as the mean ± SEM. One-way ANOVA was adopted for statistical analysis. \*,  $P < 0.05$ ; \*\*,  $P < 0.01$ ; \*\*\*,  $P < 0.001$  compared with the model group ( $n = 6$ ). SOD, superoxide dismutase; MDA, malondialdehyde; NO, nitric oxide; iNOS, inducible nitric oxide synthase; IHC-P, immunohistochemical and chemical staining-paraffin sections; COPD, chronic obstructive pulmonary disease; prot, protein; SEM, standard error of the mean; ANOVA, analysis of variance.

development and involves a variety of inflammatory cells, cytokines, and inflammatory mediators (19). Compared with the control group, the COPD rats showed increased TNF- $\alpha$ , IL-1 $\beta$ , and IL-4 levels in the serum, and all of these inflammatory factors could be reduced by halotherapy treatment (Figure 4A-4C). CD4<sup>+</sup> T cells mediate COPD autoimmune responses by promoting immunoglobulin G (IgG) production (20), while cytotoxic perforin and granzyme B secretion by CD8<sup>+</sup> T cells (21) leads to cell death and apoptosis. Thus, we detected the CD4<sup>+</sup> and CD8<sup>+</sup> T cells in the blood of the rats. The flow cytometry results showed that compared with the control group, the CD4<sup>+</sup> and CD8<sup>+</sup> T cells in the blood of COPD rats were significantly increased, which decreased after halotherapy treatment (Figure 4D-4G).

#### **Halotherapy inhibits the NLRP3 signaling pathway to reduce pyroptosis in COPD rats**

The NLRP3/ASC/Caspase-1 pathway has been shown to play an important role in the cigarette smoke-

induced pyroptosis of bronchial epithelial cells. Toll-like receptors (TLRs) are responsible for the detection and recognition of pattern recognition receptors (PRRs), not only exogenous pathogen-associated molecular patterns (PAMPs) but also endogenous damage-associated molecular patterns (DAMPs). The Western blot results showed that cigarette smoke-induced COPD rats displayed increased TLR4, NF- $\kappa$ B, and GSDMD protein expression levels in the lungs; however, after halotherapy treatment, the TLR4 and NF- $\kappa$ B protein expression levels in the lungs of COPD rats decreased markedly (Figure 5A). The expression of GSDMD was decreased but did not show a notable trend.

Oxidative stress can promote the expression of NLRP3 by activating the NF- $\kappa$ B signaling pathway, which in turn leads to the activation of the NLRP3 inflammasome. The Western blot results also showed that cigarette smoke-induced COPD rats exhibited increased NLRP3, ASC, and Caspase-1 protein expression levels in the lungs; meanwhile, after halotherapy treatment, the NLRP3, ASC, and Caspase-1 protein expression in the lungs of



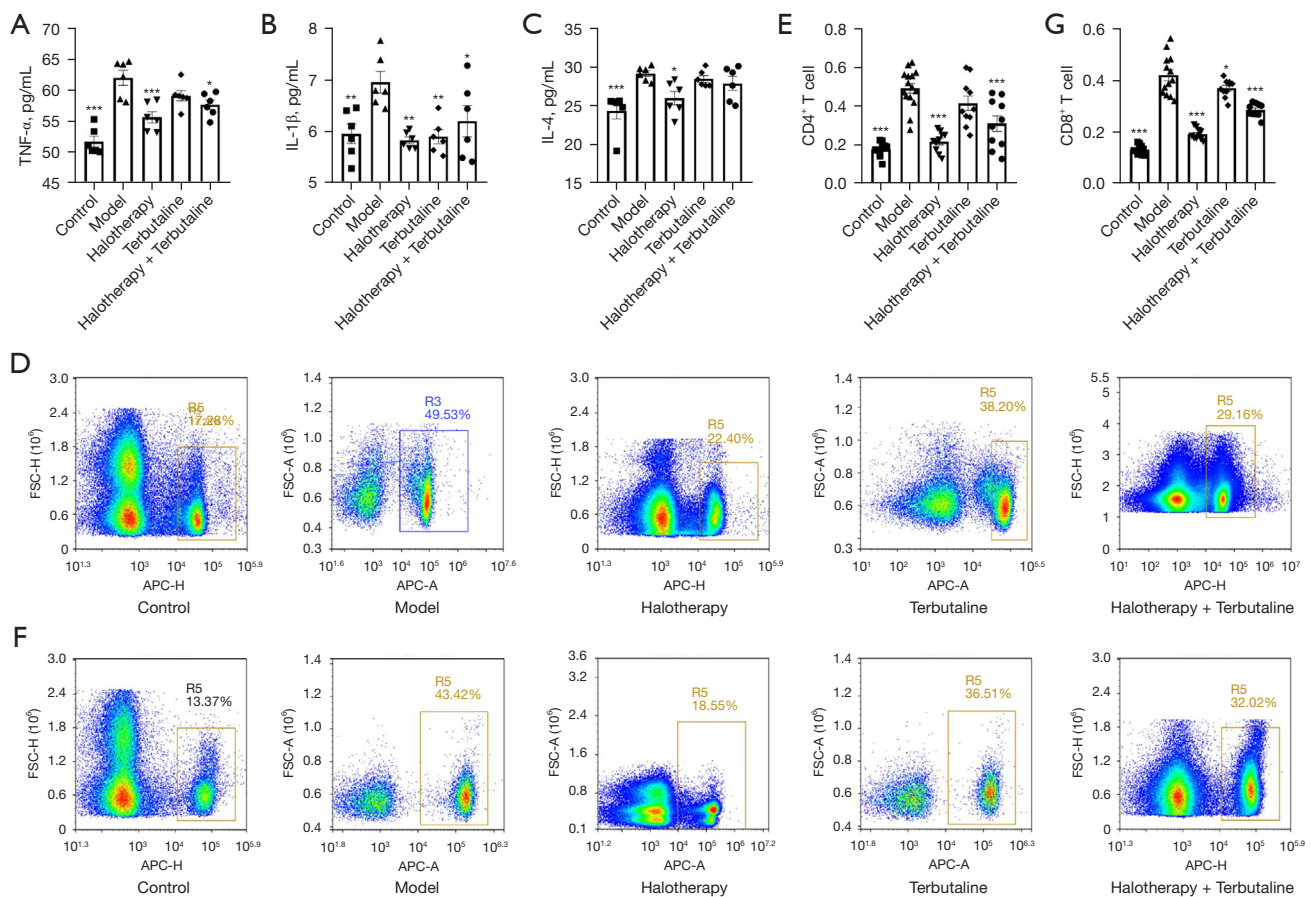
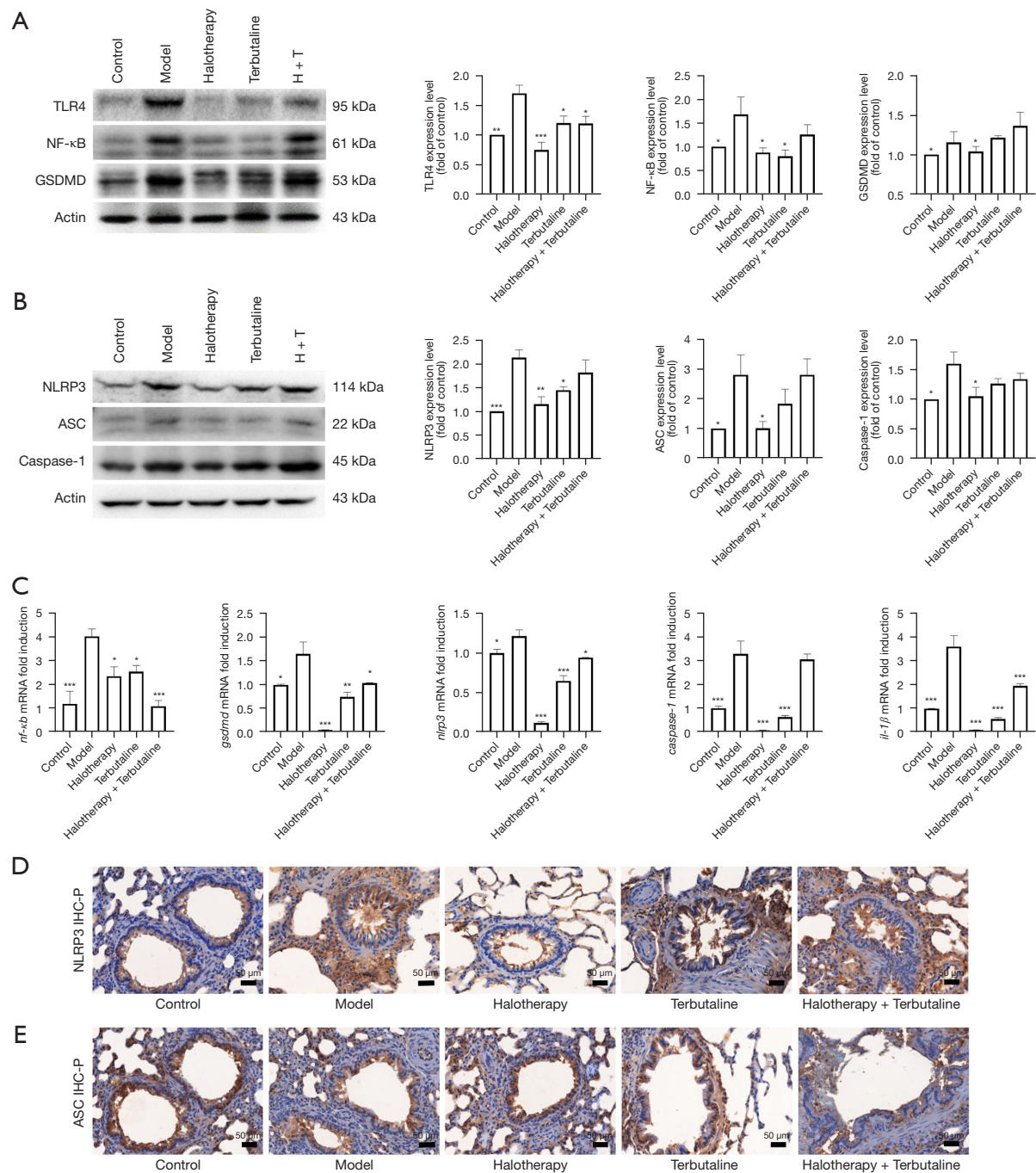


**Figure 4** Halotherapy alleviates inflammation and the immune response in COPD rats. Serum TNF- $\alpha$  (A), IL-1 $\beta$  (B), and IL-4 (C) levels were detected using ELISA kits. The levels of CD4<sup>+</sup> T cells in the blood were detected (D) and quantified (E) by flow cytometry. The levels of CD8<sup>+</sup> T cells in the blood were detected (F) and quantified (G) by flow cytometry. Data are expressed as the mean  $\pm$  SEM. One-way ANOVA was adopted for statistical analysis. \*, P<0.05; \*\*, P<0.01; \*\*\*, P<0.001 compared with the model group. In (A-D), n=6. In (E-G), n=13 in the model group, n=10 in the other groups. TNF- $\alpha$ , tumor necrosis factor  $\alpha$ ; IL, interleukin; FSC-H, forward scatter height; APC-H, allophycocyanin height; FSC-A, forward scatter area; APC-A, allophycocyanin area; COPD, chronic obstructive pulmonary disease; ELISA, enzyme-linked immunosorbent assay; SEM, standard error of the mean; ANOVA, analysis of variance.

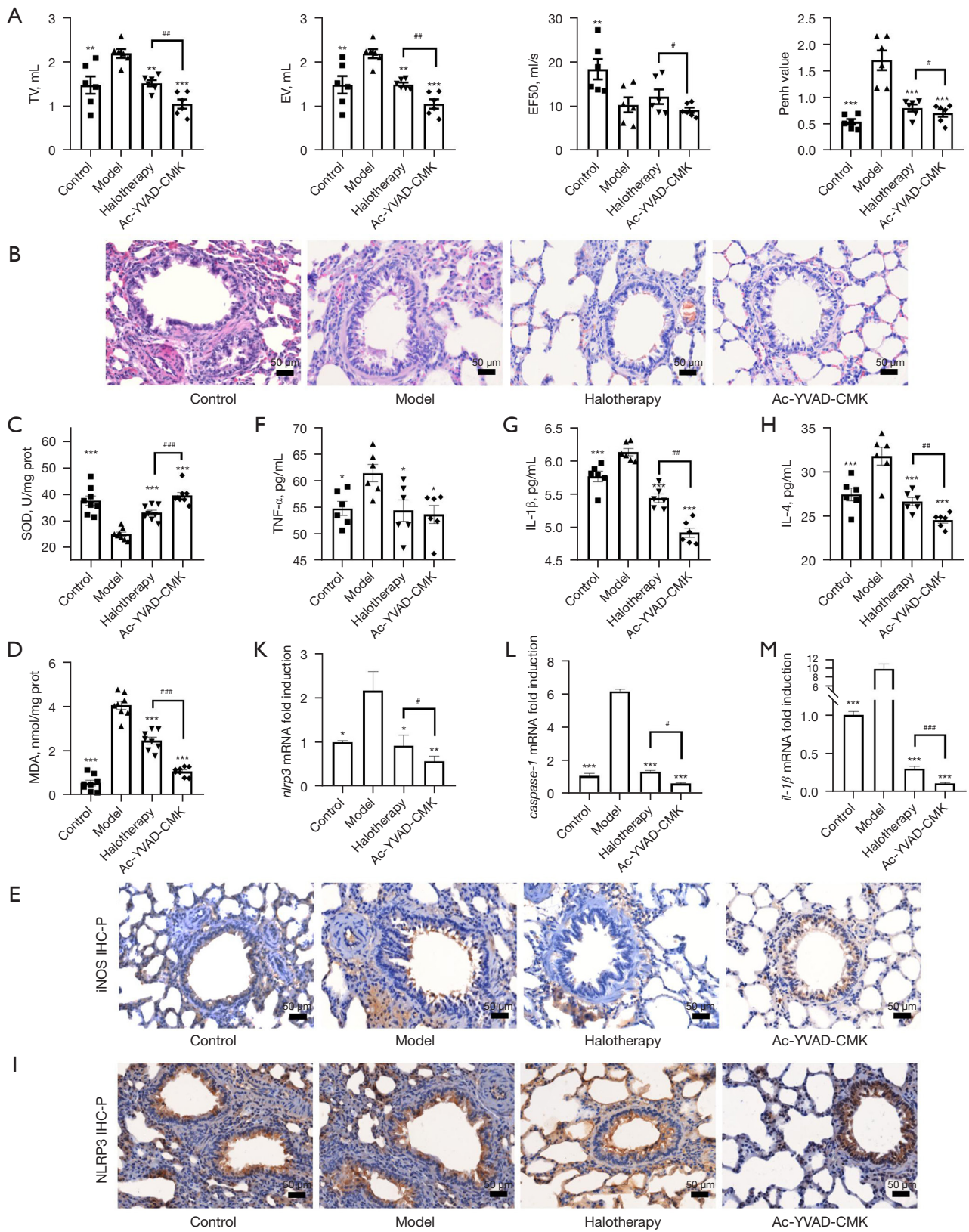
COPD rats decreased significantly (Figure 5B). The mRNA expression levels of NF- $\kappa$ B, GSDMD, NLRP3, Caspase-1, and IL-1 $\beta$  in lung tissue were detected by PCR, and all of the mRNA expression levels showed similar changes to the protein expression levels in the lungs of COPD rats (Figure 5C). The NLRP3 and ASC protein expression levels were also detected by immunohistochemistry staining; the COPD rats showed more positive staining area of NLRP3 and ASC in the lungs compared to the control groups. Halotherapy treatment reduced the positive staining area of NLRP3 and ASC in the lungs of COPD rats (Figure 5D,5E).

### *The Caspase-1 inhibitor extracts the therapeutic effect on COPD rats*

Ac-YVAD-CMK, a selective inhibitor of Caspase-1, has been widely studied in cerebral hemorrhage (22), acute gastric injury (23), and sepsis-induced acute kidney injury (24). However, research on Ac-YVAD-CMK in COPD has not yet been reported. Therefore, the Caspase-1 inhibitor Ac-YVAD-CMK was applied to the COPD rats, and we compared the therapeutic effect of halotherapy and Ac-YVAD-CMK in COPD rats. The lung function and pathological changes were measured



**Figure 5** Halotherapy inhibits the NLRP3 signaling pathway to reduce pyroptosis in COPD rats. TLR4, NF- $\kappa$ B, and GSDMD protein expression in the lung tissue homogenates were detected by Western blot (A). NLRP3, ASC, and Caspase-1 protein expression in the lung tissue homogenates were detected by Western blot (B). *nf- $\kappa$ b*, *gsdmd*, *nlrp3*, *caspase-1*, and *il-1 $\beta$*  mRNA expression levels in the lung tissue were detected by PCR (C). The expression and location of NLRP3 (D) and ASC (E) in the lung tissues were detected by immunohistochemistry (scale bar, 50  $\mu$ m). Data are expressed as the mean  $\pm$  SEM. One-way ANOVA was adopted for statistical analysis. \*,  $P < 0.05$ ; \*\*,  $P < 0.01$ ; \*\*\*,  $P < 0.001$  compared with the model group ( $n = 4$ ). TLR4, Toll-like receptor 4; NF- $\kappa$ B, nuclear factor kappa B; GSDMD, gasdermin-D; NLRP3, nucleotide-binding oligomerization domain-like receptor protein 3; ASC, apoptosis-associated speck-like protein containing a C-terminal caspase recruitment domain; IL-1 $\beta$ , interleukin 1 $\beta$ ; H + T, halotherapy + terbutaline; IHC-P, immunohistochemical and chemical staining-paraffin sections; COPD, chronic obstructive pulmonary disease; SEM, standard error of the mean; ANOVA, analysis of variance.



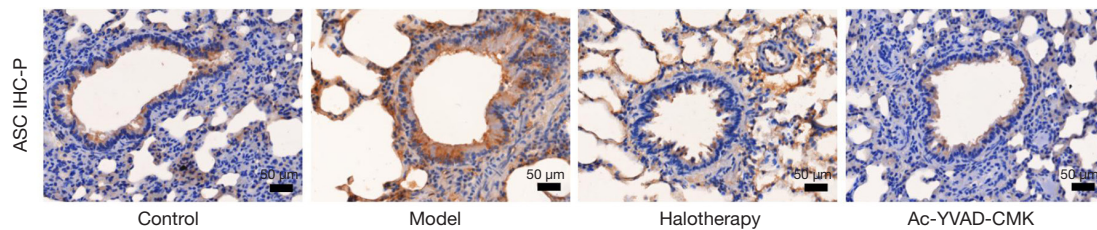


**Figure 6** The Caspase-1 inhibitor enhanced the therapeutic effect of halotherapy in COPD rats. (A) The following indexes were recorded by pulmonary function test: TV, EV, EF50, and Penh. (B) Pulmonary histology was detected by H&E staining (scale bar, 50  $\mu\text{m}$ ). SOD (C) and MDA (D) levels in the lung tissue homogenates were detected using a biochemical kit. (E) The expression and location of iNOS in lung tissues were detected by immunohistochemistry (scale bar, 50  $\mu\text{m}$ ). Serum TNF- $\alpha$  (F), IL-1 $\beta$  (G), and IL-4 (H) levels were detected using ELISA kits. The expression and location of NLRP3 (I) and ASC (J) in lung tissues were detected by immunohistochemistry (scale bar, 50  $\mu\text{m}$ ). *nlrp3* (K), *caspase-1* (L), and *il-1 $\beta$*  (M) mRNA expression levels in the lung tissue were detected by PCR. Data are expressed as the mean  $\pm$  SEM. One-way ANOVA was adopted for statistical analysis. \*,  $P < 0.05$ ; \*\*,  $P < 0.01$ ; \*\*\*,  $P < 0.001$  compared with the model group. #,  $P < 0.05$ ; ##,  $P < 0.01$ ; ###,  $P < 0.001$ . TV, tidal volume; EV, expiratory volume; EF50, 50% exhaled volume flow rate; Penh, enhanced pause; SOD, superoxide dismutase; TNF- $\alpha$ , tumor necrosis factor  $\alpha$ ; IL, interleukin; MDA, malondialdehyde; NLRP3, nucleotide-binding oligomerization domain-like receptor protein 3; ASC, apoptosis-associated speck-like protein containing a C-terminal caspase recruitment domain; COPD, chronic obstructive pulmonary disease; iNOS, inducible nitric oxide synthase; IHC-P, immunohistochemical and chemical staining-paraffin sections; ELISA, enzyme-linked immunosorbent assay; prot, protein; SEM, standard error of the mean; ANOVA, analysis of variance.

in the COPD rats; both halotherapy and Ac-YVAD-CMK improved the lung function and pathological changes of the lungs of COPD rats (Figure 6A,6B). Like halotherapy, Ac-YVAD-CMK increased the SOD activity and decreased MDA levels in the lungs of COPD rats (Figure 6C,6D). Immunohistochemical staining showed that the iNOS protein expression in the lungs of COPD rats was decreased by halotherapy or Ac-YVAD-CMK treatment (Figure 6E). Moreover, Ac-YVAD-CMK decreased the serum TNF- $\alpha$ , IL-1 $\beta$ , and IL-4 levels in COPD rats, which is consistent with halotherapy treatment (Figure 6F-6H). The NLRP3 and ASC immunohistochemistry staining results showed that halotherapy and Ac-YVAD-CMK both reduced the positive staining area of NLRP3 and ASC in the lungs of COPD rats (Figure 6I,6J). Moreover, the NLRP3, Caspase-1, and IL-1 $\beta$  mRNA results showed that halotherapy and Ac-YVAD-CMK both reduced NLRP3, Caspase-1, and IL-1 $\beta$  mRNA expression in the lungs of COPD rats (Figure 6K-6M)

## Discussion

COPD is a common respiratory disease that occurs mostly in elderly individuals, with high rates of prevalence and mortality. The currently available clinical drugs cannot

prevent the progressive decline of lung function, the quality of life of patients is greatly limited, and there are considerable social and mental burdens as well as economic pressures.

In Eastern Europe, natural salt caves have been used to help relieve the symptoms of chest conditions. The temperature inside the cave is stable, the humidity is moderate, and it is rich in fine aerosol elements (sodium, potassium, magnesium, and calcium) and devoid of air pollutants and allergens (25). Natural crystalline salts are inhaled via aerosols or directly from the environment to promote respiration and breathing. Halotherapy builds on this premise (26). In the present study, we explored the therapeutic effect and potential mechanism of halotherapy using a COPD rat model and provided experimental evidence for the clinical application of halotherapy.

COPD is mainly characterized by progressive ventilator obstruction and/or irreversible narrowing of the bronchi, and eventually, the loss of lung tissue elasticity (27). In this study, we first observed smoking rats representative COPD symptoms. Respiratory function is considered to be an important indicator to evaluate the severity of the disease and observe the therapeutic effect. In this study, we observed a significant improvement in lung function in COPD rats after halotherapy. Recovery was also observed

at the gross level of lung tissue.

Long-term smoking is the most important risk factor for COPD (3) and a major cause of oxidative stress as well as inflammatory and immune responses. Cigarette smoke contains harmful substances such as nicotine, tar, and cadmium, which stimulate the generation of a large number of oxygen free radicals, increase the secretion of inflammatory factors and elastase, and lead to chronic inflammatory changes in the airways, lung parenchyma, and pulmonary vessels (28). And it eventually leads to the development of COPD (13). According to the latest report (29), inflammatory damage to the airway epithelium exposed to cigarette smoke is amplified by oxidative stress cascades. As we detected, halotherapy showed a protective effect in cigarette-smoking rats by upregulating SOD activity and downregulating MDA levels against cigarette smoke-induced oxidative stress. Simultaneously, halotherapy also significantly rescued the accumulation of inflammatory factors in the serum of COPD rats and reduced the activation of T lymphocytes. We selected terbutaline, a frequently-used clinical prescription, as the positive control group. It is a bronchodilator that also appears to improve respiratory function in COPD rats. But it does not have a good performance in oxidative stress and inflammation.

In recent years, pyroptosis has been a research hotspot in programmed death, which is generally triggered by pathogenic antigens and stimulatory signals *in vitro* and *in vivo* (30). The activated signals promote the release of inflammatory factors into the blood circulation accompanied by apoptosis (31). Reducing cell damage and death in COPD has always been a major goal of treatment. NLRP3, ASC, and Caspase-1 together constitute the inflammasome. The activation of NLRP3 initiates the pyroptosis signaling pathway mediating the inflammatory response. ASC, as an intermediate component of the pyroptosis signaling pathway, is highly expressed in macrophages. When cells are stimulated, ASC becomes an adaptor protein for Caspase-1 and the two aggregate with each other through signaling. In turn, Caspase-1 produces the most critical inflammatory mediators. The released chemokines and proinflammatory factors lead to a cascade of inflammatory reactions that promote corresponding immune effects, which is the

classical NLRP3 inflammasome pathway (32,33). Their roles in COPD have been reported previously (34,35). Consistent with our results, halotherapy exerted therapeutic effects by downregulating the expression of the NLRP3/ASC/Caspase-1 signaling pathway in COPD rats. To some extent, inhibitors counteracted the therapeutic effect of halotherapy. This illustrates that the NLRP3 inflammasome is a potential target for halotherapy to exert anti-inflammatory, anti-oxidative stress as well as anti-pyroptosis effects. This adds an alternative target for clinical use to treat COPD.

There are still some limitations in this study that should be noted. For example, the study of the NLRP3/ASC/Caspase-1 signaling pathway was not thoroughly verified by gene knockout. Subsequent experiments will use this as a basis for genetic exploration. The experiments in rats laid the foundation for the next clinical studies and provided references for practical applications. In subsequent experiments, it is necessary to further combine this with clinical practice to compare the changes in the inflammatory response, oxidative stress, and pyroptosis in patients with different stages of COPD treated with halotherapy and other treatments.

In summary, this study employed halotherapy to treat rats exposed to cigarette smoke and demonstrate that halotherapy can improve lung function by inhibiting the NLRP3/ASC/Caspase-1 signaling pathway, reducing inflammation and pyroptosis in COPD rats (*Figure 7*). Halotherapy provides a new option for the prevention and treatment of COPD; however, the deep therapeutic mechanism of halotherapy is still worthy of further study.

## Conclusions

It has been experimentally demonstrated that halotherapy can ameliorate lung morphological structure, improve lung function, and inhibit inflammatory response, oxidative stress, immune response, and pyroptosis in a rat model of COPD. Halotherapy aims to repair airway injury by abolishing the inflammatory response and pyroptosis by inhibiting the expression of the NLRP3/ASC/Caspase-1 pathway.

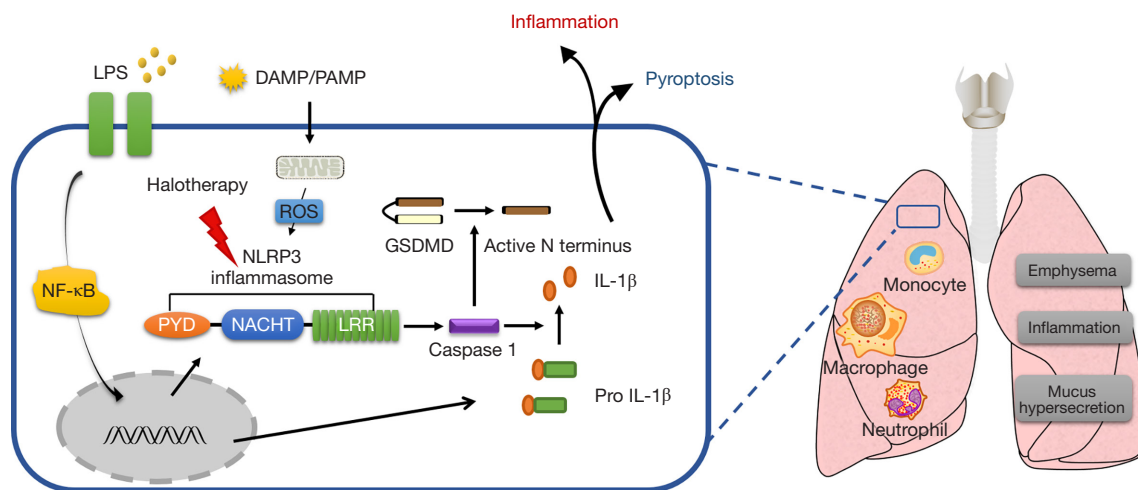


**Figure 7** When COPD occurs, there will be emphysema, inflammation and mucus hypersecretion, which are closely related to monocytes, macrophages and neutrophils. NLRP3 inflammatory corpuscle-induced pyroptosis is also involved. Halotherapy achieves therapeutic effects in COPD by inhibiting NLRP3 inflammasome. LPS, lipopolysaccharide; DAMP, damage-associated molecular patterns; PAMP, pathogen-associated molecular patterns; ROS, reactive oxygen species; NLRP3, nucleotide-binding oligomerization domain-like receptor protein 3; GSDMD, gasdermin-D; IL-1 $\beta$ , interleukin 1 $\beta$ ; NF- $\kappa$ B, nuclear factor  $\kappa$ B.

## Acknowledgments

**Funding:** This work was sponsored by the General Project of Jiangsu Provincial Health Commission (No. H2019029), the Jiangsu Province Six One Project (No. LGY2018054), the “Six Talent Peaks” High-Level Talents Level B (No. WSN-015), and the 333 High-Level Personnel Training Program.

## Footnote

**Reporting Checklist:** The authors have completed the ARRIVE reporting checklist. Available at <https://atm.amegroups.com/article/view/10.21037/atm-22-5632/rc>

**Data Sharing Statement:** Available at <https://atm.amegroups.com/article/view/10.21037/atm-22-5632/dss>

**Conflicts of Interest:** All authors have completed the ICMJE uniform disclosure form (available at <https://atm.amegroups.com/article/view/10.21037/atm-22-5632/coif>). X Shen is from Nanjing Kuancheng Technology Co., Ltd. The other authors have no conflicts of interest to declare.

**Ethical Statement:** The authors are accountable for all aspects of the work in ensuring that questions related to the accuracy or integrity of any part of the work are

appropriately investigated and resolved. This study was conducted in accordance with internationally accepted animal welfare guidelines and passed the ethics review of Nanjing University of Chinese Medicine (No. 202007A015).

**Open Access Statement:** This is an Open Access article distributed in accordance with the Creative Commons Attribution-NonCommercial-NoDerivs 4.0 International License (CC BY-NC-ND 4.0), which permits the non-commercial replication and distribution of the article with the strict proviso that no changes or edits are made and the original work is properly cited (including links to both the formal publication through the relevant DOI and the license). See: <https://creativecommons.org/licenses/by-nc-nd/4.0/>.

## References

- Salvi S. Tobacco smoking and environmental risk factors for chronic obstructive pulmonary disease. *Clin Chest Med* 2014;35:17-27.
- Alqahtani JS, Aquilina J, Bafadhel M, et al. Research priorities for exacerbations of COPD. *Lancet Respir Med* 2021;9:824-6.
- Khoo EM, Li D, Ungan M, et al. Lung health in LMICs: tackling challenges ahead. *Lancet* 2021;398:488-9.

4. Domej W, Oettl K, Renner W. Oxidative stress and free radicals in COPD--implications and relevance for treatment. *Int J Chron Obstruct Pulmon Dis* 2014;9:1207-24.
5. Lopez AD, Shibuya K, Rao C, et al. Chronic obstructive pulmonary disease: current burden and future projections. *Eur Respir J* 2006;27:397-412.
6. López-Campos JL, Tan W, Soriano JB. Global burden of COPD. *Respirology* 2016;21:14-23.
7. Rhee CK, Chau NQ, Yunus F, et al. Management of COPD in Asia: A position statement of the Asian Pacific Society of Respirology. *Respirology* 2019;24:1018-25.
8. Celli BR, Anderson JA, Cowans NJ, et al. Pharmacotherapy and Lung Function Decline in Patients with Chronic Obstructive Pulmonary Disease. A Systematic Review. *Am J Respir Crit Care Med* 2021;203:689-98.
9. Olschewski H, Buhl R, Funk GC, et al. Chronic obstructive pulmonary disease: the right treatment for the right patient. *Internist (Berl)* 2021;62:679-85.
10. Chervinskaya AV, Kotenko KV. Efficiency of controlled halotherapy in rehabilitation of patients with occupational lung diseases. *Med Tr Prom Ekol* 2016;(11):38-40.
11. Barber D, Malyshev Y, Oluyadi F, et al. Halotherapy for Chronic Respiratory Disorders: From the Cave to the Clinical. *Altern Ther Health Med* 2022;28:52-6.
12. Zhang MY, Jiang YX, Yang YC, et al. Cigarette smoke extract induces pyroptosis in human bronchial epithelial cells through the ROS/NLRP3/caspase-1 pathway. *Life Sci* 2021;269:119090.
13. Nikota JK, Stämpfli MR. Cigarette smoke-induced inflammation and respiratory host defense: Insights from animal models. *Pulm Pharmacol Ther* 2012;25:257-62.
14. Shu J, Li D, Ouyang H, et al. Comparison and evaluation of two different methods to establish the cigarette smoke exposure mouse model of COPD. *Sci Rep* 2017;7:15454.
15. Tanner L, Single AB. Animal Models Reflecting Chronic Obstructive Pulmonary Disease and Related Respiratory Disorders: Translating Pre-Clinical Data into Clinical Relevance. *J Innate Immun* 2020;12:203-25.
16. Zheng H, Liu Y, Huang T, et al. Development and characterization of a rat model of chronic obstructive pulmonary disease (COPD) induced by sidestream cigarette smoke. *Toxicol Lett* 2009;189:225-34.
17. Holownia A, Mroz RM, Wielgat P, et al. Altered histone deacetylase activity and iNOS expression in cells isolated from induced sputum of COPD patients treated with tiotropium. *Adv Exp Med Biol* 2013;788:1-6.
18. Bayarri MA, Milara J, Estornut C, et al. Nitric Oxide System and Bronchial Epithelium: More Than a Barrier. *Front Physiol* 2021;12:687381.
19. Celli BR. Predictors of mortality in COPD. *Respir Med* 2010;104:773-9.
20. Gadgil A, Duncan SR. Role of T-lymphocytes and pro-inflammatory mediators in the pathogenesis of chronic obstructive pulmonary disease. *Int J Chron Obstruct Pulmon Dis* 2008;3:531-41.
21. Barnes PJ. Inflammatory mechanisms in patients with chronic obstructive pulmonary disease. *J Allergy Clin Immunol* 2016;138:16-27.
22. Lin X, Ye H, Siaw-Debrah F, et al. AC-YVAD-CMK Inhibits Pyroptosis and Improves Functional Outcome after Intracerebral Hemorrhage. *Biomed Res Int* 2018;2018:3706047.
23. Zhang F, Wang L, Wang JJ, et al. The caspase-1 inhibitor AC-YVAD-CMK attenuates acute gastric injury in mice: involvement of silencing NLRP3 inflammasome activities. *Sci Rep* 2016;6:24166.
24. Yang M, Fang JT, Zhang NS, et al. Caspase-1-Inhibitor AC-YVAD-CMK Inhibits Pyroptosis and Ameliorates Acute Kidney Injury in a Model of Sepsis. *Biomed Res Int* 2021;2021:6636621.
25. Chervinskaya AV, Zilber NA. Halotherapy for treatment of respiratory diseases. *J Aerosol Med* 1995;8:221-32.
26. Rashleigh R, Smith SM, Roberts NJ. A review of halotherapy for chronic obstructive pulmonary disease. *Int J Chron Obstruct Pulmon Dis* 2014;9:239-46.
27. Celli BR, Fabbri LM, Aaron SD, et al. An Updated Definition and Severity Classification of Chronic Obstructive Pulmonary Disease Exacerbations: The Rome Proposal. *Am J Respir Crit Care Med* 2021;204:1251-8.
28. David B, Bafadhel M, Koenderman L, et al. Eosinophilic inflammation in COPD: from an inflammatory marker to a treatable trait. *Thorax* 2021;76:188-95.
29. Cipollina C, Bruno A, Fasola S, et al. Cellular and Molecular Signatures of Oxidative Stress in Bronchial Epithelial Cell Models Injured by Cigarette Smoke Extract. *Int J Mol Sci* 2022;23:1770.
30. Shi J, Gao W, Shao F. Pyroptosis: Gasdermin-Mediated Programmed Necrotic Cell Death. *Trends Biochem Sci* 2017;42:245-54.
31. Jorgensen I, Miao EA. Pyroptotic cell death defends against intracellular pathogens. *Immunol Rev* 2015;265:130-42.
32. Kelley N, Jeltema D, Duan Y, et al. The NLRP3 Inflammasome: An Overview of Mechanisms of Activation and Regulation. *Int J Mol Sci* 2019;20:3328.

33. He Y, Hara H, Núñez G. Mechanism and Regulation of NLRP3 Inflammasome Activation. *Trends Biochem Sci* 2016;41:1012-21.
34. Tian X, Xue Y, Xie G, et al. (-)-Epicatechin ameliorates cigarette smoke-induced lung inflammation via inhibiting ROS/NLRP3 inflammasome pathway in rats with COPD. *Toxicol Appl Pharmacol* 2021;429:115674.
35. Mahalanobish S, Dutta S, Saha S, et al. Melatonin induced suppression of ER stress and mitochondrial dysfunction inhibited NLRP3 inflammasome activation in COPD mice. *Food Chem Toxicol* 2020;144:111588.

(English Language Editor: A. Kassem)

**Cite this article as:** Zhang C, Zhu W, Meng Q, Lian N, Wu J, Liu B, Wang H, Wang X, Gu S, Wen J, Shen X, Li Y, Qi X. Halotherapy relieves chronic obstructive pulmonary disease by alleviating NLRP3 inflammasome-mediated pyroptosis. *Ann Transl Med* 2022;10(23):1279. doi: 10.21037/atm-22-5632